

## Effects of Clodronate on Cancer Growth and $Ca^{2+}$ Signaling of Human Thyroid Carcinoma Cell Lines

DE-MING YANG<sup>1\*</sup>, CHIN-WEN CHI<sup>1,5\*</sup>, HWEY-MAY CHANG<sup>2</sup>, LI-HWA WU<sup>2</sup>,  
TING-KUEI LEE<sup>2</sup>, JEN-DER LIN<sup>3</sup>, SZU-TAH CHEN<sup>3</sup> and CHEN-HSEN LEE<sup>4</sup>

Departments of <sup>1</sup>Medical Research and Education, <sup>2</sup>Experimental Surgery and  
<sup>4</sup>Surgery, Taipei Veterans General Hospital, Taipei, Taiwan;

<sup>3</sup>Department of Endocrinology and Metabolism, Chang Gung Memorial Hospital, Taoyuan;

<sup>5</sup>Institute of Pharmacology, School of Medicine, National Yang-Ming University,  
Taipei, Taiwan, Republic of China

**Abstract.** Clodronate, one of the halogenated bisphosphonates, was found to inhibit the cell growth of endocytic macrophages, osteoclasts and several cancer cells through diverse mechanisms. Cytosolic  $Ca^{2+}$  signaling had previously been suggested as an apoptotic signal to certain cancer cells. Whether clodronate has an anti-cancer effect and induces the  $Ca^{2+}$  signal in thyroid cancer cells remains unknown. In this study, the effects of clodronate, including growth inhibition and cytosolic  $Ca^{2+}$  signaling, were examined and analyzed on ARO, SW579, WRO and TT thyroid cancer cell lines. Clodronate decreased the growth of these cells in a dose-dependent manner and was more effective on slow growing cells. Clodronate treatment transiently increased cytosolic  $Ca^{2+}$  on slow growing SW579 thyroid cancer cells but not on the fast growing ARO cells. The results from this study implied that clodronate-mediated cell growth inhibition in slow growing thyroid cancer cells might correlate with a  $Ca^{2+}$  signaling pathway.

Clodronate was found to reduce the incidence of new skeletal metastases in women with breast cancer (1). This kind of halogenated biphosphonate has been widely used in the therapy of metabolic bone diseases and bone metastases (2,3). It induced cell apoptosis of osteoclasts (4), macrophages (5) and breast cancer cells (6) *in vitro*. In osteoclasts or macrophages, clodronate was metabolized

\*De-Ming Yang and Chin-Wen Chi contributed equally to this work.

Correspondence to: Chen-Hsen Lee, M.D., Department of Surgery, Taipei Veterans General Hospital, Taipei 11217, Taiwan, Republic of China. Tel: 886-2-2875-7555, Fax: 886-2-2873-8013, e-mail: chlee@vghtpe.gov.tw

**Key Words:** Clodronate, bisphosphonates, thyroid cancer cells, growth inhibition, calcium signaling.

into non-hydrolysable ATP analogs (7-9). It was therefore proposed that this clodronate metabolite competitively inhibited mitochondrial ADP/ATP translocase and then induced cell apoptosis of osteoclasts (10). At present, it is not known whether clodronate has anti-cancer activity on other cancer cells such as thyroid cancer cells.

Cytosolic  $Ca^{2+}$  ( $[Ca^{2+}]_i$ ) is a multifunctional signal for different cell types and is involved in a variety of cellular pathways (11), including regulating exocytosis (12) and cell proliferation (13). However, variable  $Ca^{2+}$  signaling pathways in the control of cell progression and apoptosis have been the topic of several investigations (14-17). Recent reports have suggested, independently, that a decrease in the endoplasmic reticulum (ER)  $Ca^{2+}$  pool was directly correlated with the anti-cancer effects (e.g. signal for apoptosis or cell growth arrest) of drugs (18-21). Since clodronate has a  $Ca^{2+}$  chelating property similar to EGTA, it would be interesting to examine the effect of clodronate on the  $[Ca^{2+}]_i$  of cancer cells and its correlation with growth inhibition activity.

In this study, we examined the effects of clodronate on the proliferation, cell morphology and  $[Ca^{2+}]_i$  of ARO, SW579, WRO and TT human thyroid cancer cell lines. The potential mechanisms of the clodronate-mediated growth inhibition and  $Ca^{2+}$  signaling were discussed.

### Materials and Methods

**Materials.** Clodronate was purchased from Leiras Oy (Turku, Finland) or Sigma Chemical Company (St. Louis, MO, USA). The acetoxymethyl ester form (AM) of Fura-2 was purchased from Molecular Probes (Eugene, OR, USA). All other reagents were purchased from Sigma Chemical Company unless indicated.

**Cell culture.** Four human thyroid cancer cell lines were used. The poorly-differentiated ARO cells and follicular WRO cells were cultured as previously reported (22). The squamous SW579 cell

line was purchased from the American Type Culture Collection (ATCC, Rockville, MD, USA) and cultured in 90% Leibovitz's L-15 medium (Gibco, BRL, USA) with 2 mM L-glutamine and 10% fetal bovine serum (FBS). The medullary TT cell line was from ATCC and was cultured in 90% Ham's F12K medium with 2 mM L-glutamine, 1.5 g/L sodium bicarbonate and 10% FBS. The cells were cultured in plastic culture dishes (Costar, Cambridge, MA, USA) for analysis of growth. When performing  $Ca^{2+}$  imaging experiments, these cells were cultured on coverglass.

**Cell growth assay.** The cell growth assay has been described previously (23). Briefly, thyroid cancer cells were seeded in a 96-well culture dish (Costar) at a density of  $4 \times 10^3$  cells/mL and cultured overnight prior to clodronate treatment. After clodronate treatment for 24-72 hours, the medium was discarded and replaced with an equal volume (100  $\mu$ L) of fresh medium containing 0.456 mg/mL 3-[4,5-dimethylthiazol-2-yl]-2,5-diphenyl tetrazolium bromide (MTT) and incubated for 1.5 hours at 37°C in the dark. The medium was discarded and the cells were then combined with 100  $\mu$ L dimethyl sulfoxide (DMSO) to dissolve the formazan produced. Cell growth was determined by the colorimetric comparison of optical density (OD) values from a microplate reader (SpectraMax 250; Molecular Devices, Sunnyvale, CA, USA) at an absorption wavelength of 570 nm.

**Digital ratio imaging for  $[Ca^{2+}]_i$  measurement.** The  $[Ca^{2+}]_i$  assay has been described previously (24). Briefly, thyroid cancer cells ( $2 \times 10^5$ ) were grown on 22-mm poly-L-lysine-coated glass coverslips placed in 35-mm culture dishes. The cells were washed with loading buffer, containing 150 mM NaCl, 5 mM KCl, 2.2 mM  $CaCl_2$ , 1 mM  $MgCl_2$ , 5 mM glucose and 10 mM HEPES, pH 7.4. The cells were treated with 5  $\mu$ M Fura-2 AM in the loading buffer for 30 minutes at 37°C. The coverslips were washed three times in the loading buffer and then mounted in a recording chamber on the platform of an inverted microscope (IX-70, Olympus Optical Co., Ltd, Tokyo, Japan). The  $[Ca^{2+}]_i$  ratio images with excitations of 340 and 380 nm were collected every 0.5 seconds by an imaging system using a high speed cooled CCD camera (MicroMAX: 782YHS, Princeton Instruments, Roper Scientific, Inc., Trenton, NJ, USA) and a xenon lamp within a monochromator as an excitation light source (Polychrome II, T.I.L.L. Photonics, Germany) and a software Axon Image Workbench 2.0 (Axon Instruments, Foster City, CA, USA). Fura-2 fluorescence images were acquired at 510 nm emission filter with alternative excitation at 340 and 380 nm for the same exposure time. The change of  $[Ca^{2+}]_i$  was calculated as the subtraction value between the ratio (fluorescent intensity excited at 340 nm to that excited at 380 nm;  $F_{340}/F_{380}$ ) value of peak (after drug application) and that of basal level (before drug treatment).

**Drug treatment for  $[Ca^{2+}]_i$  ratio imaging.** Thyroid cancer cells were treated with clodronate under the indicated conditions. When measuring  $[Ca^{2+}]_i$  using the ratio imaging method as described above, a micropipette with a tip of 2  $\mu$ m diameter was used for delivery of a very small amount (picoliter to nanoliter) of 2 mM of clodronate locally by a 15 psi ejection pulse for 0.5 seconds (Picospritzer II, General Valve, USA). The micropipettes were pulled routinely by a glass puller (P-97, Sutter Instrument Company, Novato, CA, USA), polished by a microforge (MF-83, Narishige, Japan) and clamped by a water hydraulic micromanipulator (MHW-3,

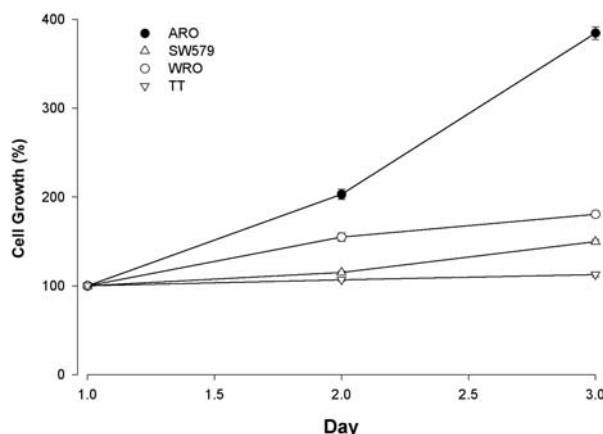


Figure 1. Comparison of cell growth rate among 4 different thyroid cancer cell lines. The growth of each thyroid cancer cell line was normalized to day 1 of respective thyroid cancer cells (ARO, ●; SW579, ○; WRO, △ and TT, ▽). As shown, ARO has the highest growth rate followed by WRO, SW579 and TT.

Narishige) that was mounted on the stage of the IX-70 inverted microscope.

**Statistical analysis.** Data are expressed as mean  $\pm$  standard error of mean (SEM) and analyzed by one-way analysis of variance or Student's *t*-test. The difference between means was considered as significant when the *p* value was  $< 0.05$ .

## Results

**Growth rate of different thyroid cancer cells.** Four different thyroid cancer cell lines were used in this study. The ARO line is a poorly-differentiated type, SW579 is squamous or spindle type, WRO is follicular type and the TT line is a medullary type. As shown in Figure 1, the growth rate of ARO was the fastest in contrast to the other slow growing cell lines. According to the proliferation profile of these 4 cell lines, the growth rate of these cells was in the order ARO > WRO > SW579 > TT.

**Clodronate inhibited proliferation of thyroid cancer cells.** Four dosages of clodronate (0.25, 0.5, 1 and 2 mM) were applied to thyroid cancer cells for 1, 2 and 3 days and the cell growth was measured by MTT assay (Figure 2). Clodronate treatment resulted in a decrease in growth of the thyroid cancer cells in a dose-dependent manner. As shown in Figure 2A, the growth of fast growing ARO cells was minimally affected by clodronate and the decrease of cell growth was not evident until day 3 after treatment with a high dose of clodronate (2 mM). On the other hand, the growth of slow growing cells stopped at 0.5 mM of clodronate. Moreover, the proliferation of these slow growing cells decreased after treatment with 1 or 2 mM of clodronate for 2 or 3 days.

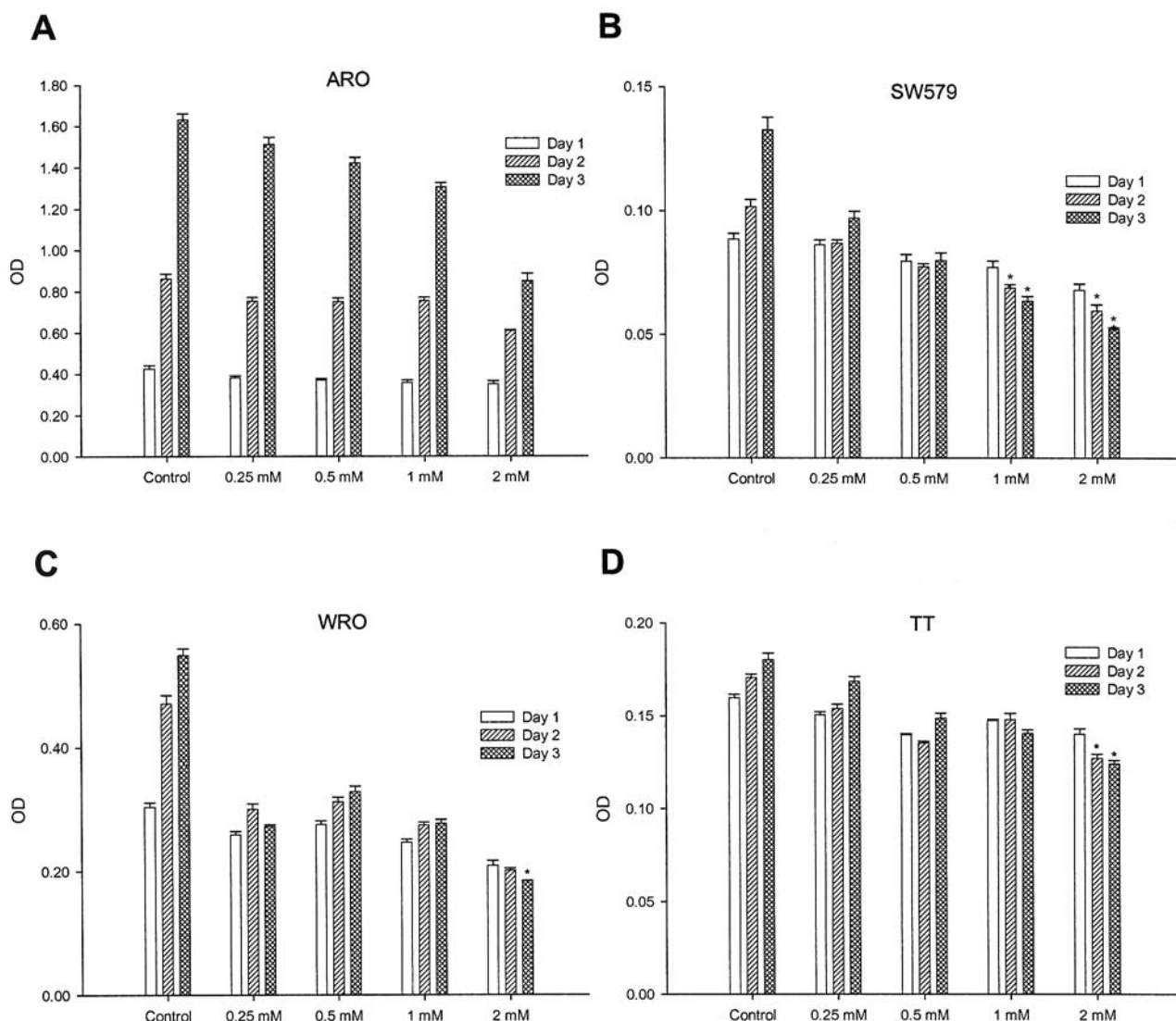


Figure 2. The effect of clodronate on cell viability of four thyroid cancer cell lines. A different dosage of clodronate (0.25, 0.5, 1 and 2 mM) was applied to these thyroid cancer cell lines (ARO, A; SW579, B; WRO, C and TT, D) for 1, 2 and 3 days. The cell viability was measured by MTT assay from three independent experiments of 6 repeated samples. Asterisks indicate  $p$  values < 0.05 compared with the day 1 group of the same dosage (one-way analysis of variance).

Differential effect of clodronate on  $[Ca^{2+}]_i$  of thyroid cancer cells. Although pretreatment of clodronate lowered the basal  $[Ca^{2+}]_i$  of most thyroid cancer cells, the response of  $[Ca^{2+}]_i$  to transiently applied clodronate in thyroid cancer cells was heterogeneous (Figure 3A-D). In ARO cells, a uniform decreased pattern of  $[Ca^{2+}]_i$  after clodronate treatment was observed (Figure 3A). In contrast, clodronate induced an increase of  $[Ca^{2+}]_i$  in the majority (>90%) of control SW579 (Figure 3B, upper panel). However, clodronate had no effect on  $[Ca^{2+}]_i$  of the majority (>90%) of SW579 cells pretreated with clodronate for 3 days (Figure 3B, lower panel). In WRO and TT cells, a differential  $[Ca^{2+}]_i$  response to clodronate was observed indicating an endogenous difference in these

cells (Figure 3C and 3D). Figure 4 shows the comparison of clodronate-induced changes in basal  $[Ca^{2+}]_i$  and  $[Ca^{2+}]_i$  in clodronate-pretreated ARO and SW579 cells. We have found that clodronate transient treatment resulted in a decrease of  $[Ca^{2+}]_i$  in ARO cells. In contrast, the same clodronate treatment induced a 20-second increase of  $[Ca^{2+}]_i$  in SW579 cells. However, after a 3-day clodronate treatment, the SW579 cells showed no  $[Ca^{2+}]_i$  response to clodronate.

## Discussion

In this study, we found that clodronate treatment increased  $[Ca^{2+}]_i$  and resulted in growth inhibition of slow growing

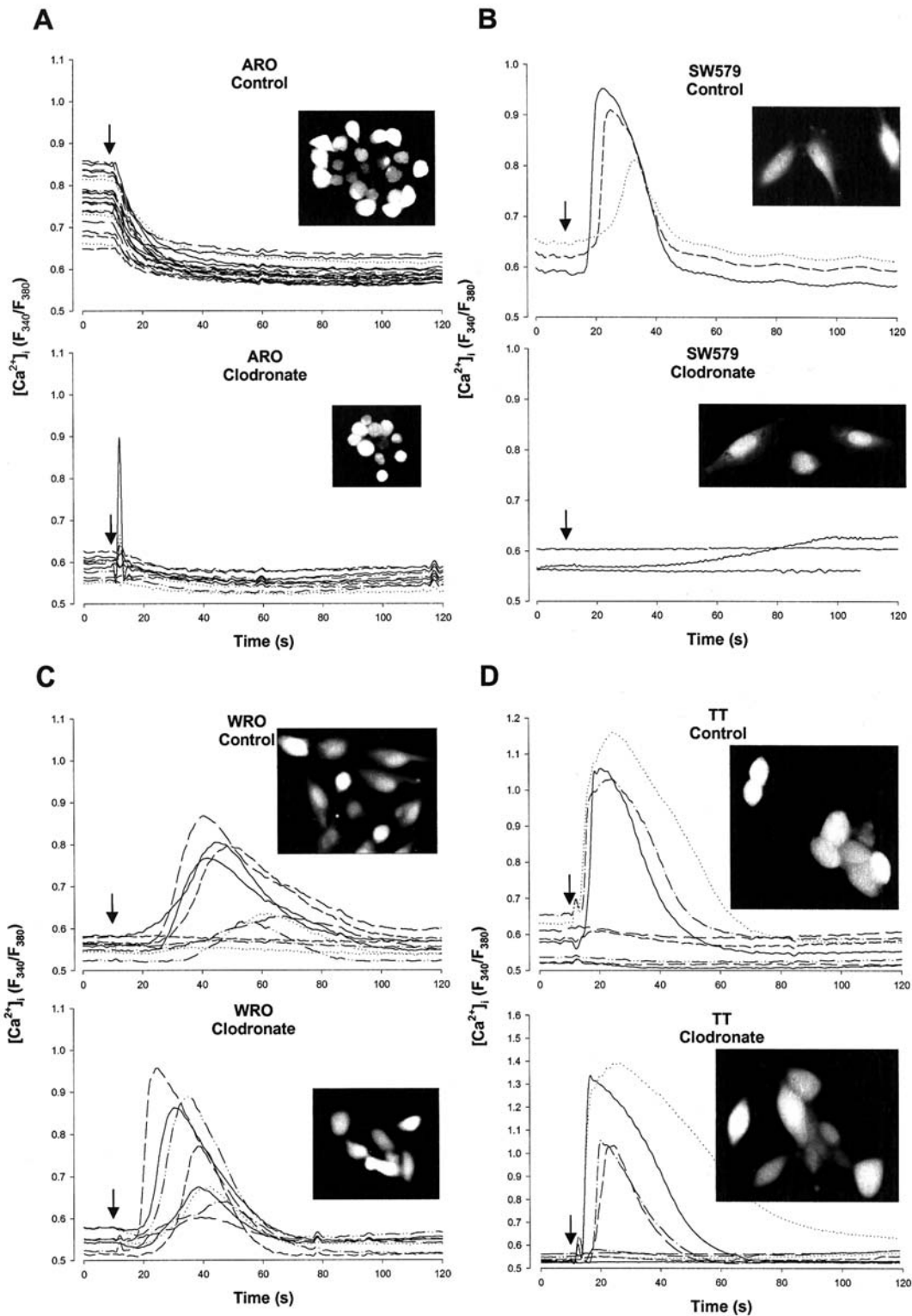


Figure 3. The effect of transient or continued clodronate treatment on the  $[Ca^{2+}]_i$  of thyroid cancer cells. The insets of each graph show the Fura-2 fluorescence images. The time-lapse changes of  $[Ca^{2+}]_i$  in 22 control and 11 pretreated ARO cells are shown in A. All the  $[Ca^{2+}]_i$  of these cells decreased when clodronate was applied transiently (as indicated by arrows, see Materials and Methods for detail). The time-lapse changes of  $[Ca^{2+}]_i$  in 3 control cells and 3 pretreated SW579 cells are shown in B. The  $[Ca^{2+}]_i$  in control SW579 cells was increased when clodronate was applied. No  $[Ca^{2+}]_i$  response in clodronate-pretreated SW579 cells was observed in the lower panel. The time-lapse changes of  $[Ca^{2+}]_i$  in 10 control cells and 8 pretreated WRO cells are shown in C, in 8 control cells and 7 pretreated TT cells are shown in D. No significant difference in the fluorescence image was found in either WRO or TT cells.

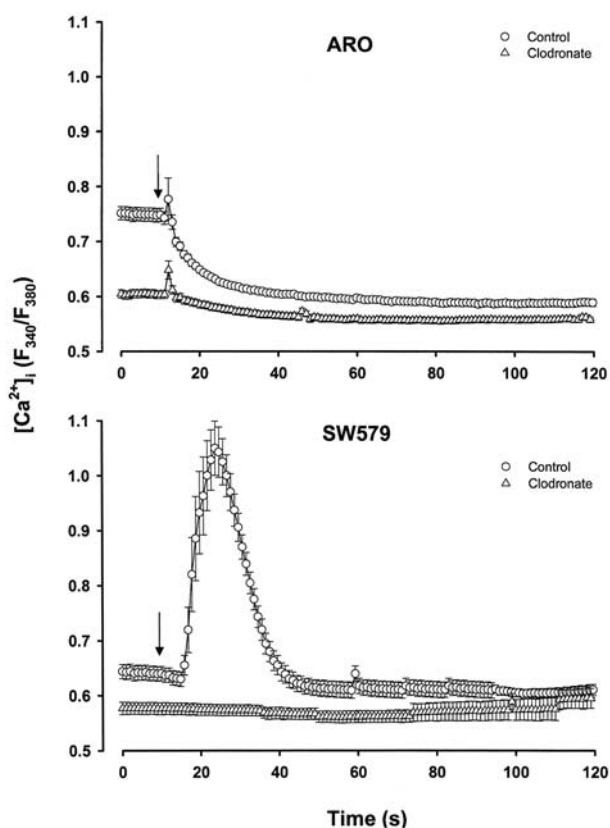


Figure 4. Comparison of averaged time-lapse  $[Ca^{2+}]_i$  response to locally applied clodronate with or without (control) clodronate pretreatment (clodronate) in ARO and SW579. The averaged signal from 34 out of ARO control and 41 out of clodronate pretreated ARO cells are shown in the ARO set. The averaged signal from 14 out of SW579 control and 8 out of SW579 clodronate pretreated cells are shown in the SW579 set.

thyroid cancer cells, but not of fast growing, poorly-differentiated ARO thyroid cancer cells.

We observed a quick response of  $[Ca^{2+}]_i$  elevation in slow growing thyroid cancer cells when clodronate was applied transiently (Figures 3 and 4). This  $[Ca^{2+}]_i$  elevation was suggested to be from a ER  $Ca^{2+}$  store (data not shown). The clodronate-induced increase of  $[Ca^{2+}]_i$  correlated well with growth inhibition in a slow growing thyroid cancer cell line, but not in fast growing ARO cells. This observation agrees well with findings that undifferentiated thyroid cancer cells have a defective ATP-induced  $Ca^{2+}$ -phosphatidylinositol (PI) signaling on IP3-linked  $Ca^{2+}$ -release process (25). In this study, we found that clodronate failed to mobilize  $[Ca^{2+}]_i$  in the poorly-differentiated ARO cells. Recently, it has been reported that a decrease in ER  $Ca^{2+}$  pool content by ATP-induced capacitative  $Ca^{2+}$  entry (CCE) induced growth arrest in human prostate cancer cells (26). It is possible that the slow growing thyroid cancer cells have a normal  $Ca^{2+}$ -PI

signaling pathway which mediated the clodronate-induced ER  $Ca^{2+}$  pool depletion or CCE.

In this study, the first transient clodronate treatment did not result in a  $[Ca^{2+}]_i$  elevation in some SW579 cells. However, these cells did respond when clodronate was applied again (data not shown). This may have resulted from insufficient clodronate or IP3 molecule to release ER  $Ca^{2+}$  during the first clodronate treatment. It is interesting that energized mitochondria might reduce the threshold concentration of IP3 which triggers CCE (27). Whether clodronate treatment modulated the threshold of IP3 is not known. More studies are needed to elucidate the detailed pathway of clodronate regulation on  $Ca^{2+}$ -IP3 and CCE signaling.

It has been suggested that mitochondria can regulate CCE through buffering mitochondrial  $Ca^{2+}$  in non-excitabile cells, such as T lymphocytes (28) and RBL cells (29). Mitochondria are located near to ER with specific functions related to buffering cytosolic  $Ca^{2+}$  (30). In a pilot study, we monitored changes in the cytosolic and the mitochondrial  $Ca^{2+}$  after a transient clodronate treatment of SW579 cells. Our results indicated that clodronate induced an increase of both the cytosolic and the mitochondrial  $Ca^{2+}$  concentration (data not shown). These results suggest that the mitochondrion participated in the buffering of the cytosolic  $Ca^{2+}$  change during a clodronate-induced  $[Ca^{2+}]_i$  increase in SW579 thyroid cancer cells.

In this study, we found that the original spindle and squamous shape of the SW579 thyroid cancer cell changed to a round or thinner shape after clodronate treatment (data not shown). Furthermore, clodronate treatment induced changes in the distribution as well as the level of F-actin in the slow growing thyroid cancer cell lines, but not the fast growing ARO cells (data not shown). Bisphosphonates were found to inhibit breast and prostate cancer cell adhesion and invasion (31,32). These results together imply that clodronate might change the organization of the cytoskeleton and cell morphology, affect cell adhesion and inhibit cell growth of thyroid SW579 cancer cells.

Regarding the anti-proliferation effect, a dose-dependent response was observed (Figure 2) and this anti-cancer effect correlated to growth arrest and a  $Ca^{2+}$ -dependent signaling. Due to the high hydrophilic property of clodronate, it has been found to be internalized into endocytic cells such as macrophage and even under liposome-capsulated status (33,34). Moreover, it has been proposed that the mechanism of clodronate-induced growth inhibition of cancer cells is apoptosis through a metabolite of clodronate (35-38). Further studies are needed to clarify whether thyroid cancer cells take up clodronate efficiently and precede apoptosis induced by its metabolite, as described before (39). In conclusion, we found that clodronate inhibited the growth of

human thyroid cancer cell lines. The clodronate-mediated growth inhibition correlated to  $\text{Ca}^{2+}$  signaling and probably morphological change.

### Acknowledgements

This study was supported by grants from the Taipei Veterans General Hospital (VGH-91-245 and VGH-91-377), Taipei, Taiwan, Republic of China. The authors would like to thank Drs. Lung-Sen Kao and Chung-Chih Lin for discussions and suggestions for the manuscript.

### References

- Diel IJ, Solomayer EF, Costa SD, Gollan C, Goerner R, Wallwiener D, Kaufmann M and Bastert G: Reduction in new metastases in breast cancer with adjuvant clodronate treatment. *N Engl J Med* 339: 357-363, 1998.
- Fleisch H: Bisphosphonates: mechanisms of action. *Endocr Rev* 19: 80-100, 1998.
- Fleisch H: Development of bisphosphonates. *Breast Cancer Res* 4: 30-34, 2002.
- Selander KS, Monkkonen J, Karhukorpi EK, Harkonen P, Hannuniemi R and Vaananen HK: Characteristics of clodronate-induced apoptosis in osteoclasts and macrophages. *Mol Pharmacol* 50: 1127-1138, 1996.
- Buiting AM, Zhou F, Bakker JA, van Rooijen N and Huang L: Biodistribution of clodronate and liposomes used in the liposome mediated macrophage 'suicide' approach. *J Immunol Methods* 192: 55-62, 1996.
- Fromigie O, Lagneaux L and Body JJ: Bisphosphonates induce breast cancer cell death *in vitro*. *J Bone Miner Res* 15: 2211-2221, 2000.
- Auriola S, Frith J, Rogers MJ, Koivuniemi A and Monkkonen J: Identification of adenine nucleotide-containing metabolites of bisphosphonate drugs using ion-pair liquid chromatography-electrospray mass spectrometry. *J Chromatogr B Biomed Sci Appl* 704: 187-195, 1997.
- Huikko K, Kotiaho T, Yli-Kauhahuoma J and Kostianen R: Electrospray ionization mass spectrometry and tandem mass spectrometry of clodronate and related bisphosphonate and phosphonate compounds. *J Mass Spectrom* 37: 197-208, 2002.
- Monkkonen H, Moilanen P, Monkkonen J, Frith JC, Rogers MJ and Auriola S: Analysis of an adenine nucleotide-containing metabolite of clodronate using ion pair high-performance liquid chromatography-electrospray ionisation mass spectrometry. *J Chromatogr B Biomed Sci Appl* 738: 395-403, 2000.
- Lehenkari PP, Kellinsalmi M, Napankangas JP, Ylitalo KV, Monkkonen J, Rogers MJ, Azhayevev A, Vaananen HK and Hassinen IE: Further insight into mechanism of action of clodronate: inhibition of mitochondrial ADP/ATP translocase by a nonhydrolyzable, adenine-containing metabolite. *Mol Pharmacol* 61: 1255-1262, 2002.
- Berridge MJ: The biology and medicine of calcium signalling. *Mol Cell Endocrinol* 98: 119-124, 1994.
- Yang DM and Kao LS: Relative contribution of the  $\text{Na}^+/\text{Ca}^{2+}$  exchanger, mitochondria and endoplasmic reticulum in the regulation of cytosolic  $\text{Ca}^{2+}$  and catecholamine secretion of bovine adrenal chromaffin cells. *J Neurochem* 76: 210-216, 2001.
- Liu SI, Chi CW, Lui WY, Mok KT, Wu CW and Wu SN: Correlation of hepatocyte growth factor-induced proliferation and calcium-activated potassium current in human gastric cancer cells. *Biochim Biophys Acta* 1368: 256-266, 1998.
- Vanden Abeele F, Skryma R, Shuba Y, Van Coppenolle F, Slomianny C, Roudbaraki M, Mauroy B, Wuytack F and Prevarskaya N: Bcl-2-dependent modulation of  $\text{Ca}^{2+}$  homeostasis and store-operated channels in prostate cancer cells. *Cancer Cell* 1: 169-179, 2002.
- Jayadev S, Petranka JG, Cheran SK, Biermann JA, Barrett JC and Murphy E: Reduced capacitative calcium entry correlates with vesicle accumulation and apoptosis. *J Biol Chem* 274: 8261-8268, 1999.
- Putney JW Jr, Broad LM, Braun FJ, Lievreumont JP and Bird GS: Mechanisms of capacitative calcium entry. *J Cell Sci* 114: 2223-2229, 2001.
- Wertz IE and Dixit VM: Characterization of calcium release-activated apoptosis of LNCaP prostate cancer cells. *J Biol Chem* 275: 11470-11477, 2000.
- Aktas H, Fluckiger R, Acosta JA, Savage JM, Palakurthi SS and Halperin JA: Depletion of intracellular  $\text{Ca}^{2+}$  stores, phosphorylation of eIF2 $\alpha$ , and sustained inhibition of translation initiation mediate the anticancer effects of clotrimazole. *Proc Natl Acad Sci USA* 95: 8280-8285, 1998.
- Palakurthi SS, Fluckiger R, Aktas H, Changolkar AK, Shahsafaei A, Harnett S, Kilic E and Halperin JA: Inhibition of translation initiation mediates the anticancer effect of the n-3 polyunsaturated fatty acid eicosapentaenoic acid. *Cancer Res* 60: 2919-2925, 2000.
- Skryma R, Mariot P, Bourhis XL, Coppenolle FV, Shuba Y, Vanden Abeele F, Legrand G, Humez S, Boilly B and Prevarskaya N: Store depletion and store-operated  $\text{Ca}^{2+}$  current in human prostate cancer LNCaP cells: involvement in apoptosis. *J Physiol* 527 Pt 1: 71-83, 2000.
- Vanoverberghe K, Mariot P, Vanden Abeele F, Delcourt P, Parys JB and Prevarskaya N: Mechanisms of ATP-induced calcium signaling and growth arrest in human prostate cancer cells. *Cell Calcium* 34: 75-85, 2003.
- Chen ST, Lin JD and Lin KH: Characterization of a thyroid hormone-mediated short-loop feedback control of TSH receptor gene in an anaplastic human thyroid cancer cell line. *J Endocrinol* 175: 459-465, 2002.
- Lin HL, Liu TY, Wu CW and Chi CW: 2-Methoxyestradiol-induced caspase-3 activation and apoptosis occurs through  $\text{G}_2/\text{M}$  arrest dependent and independent pathways in gastric carcinoma cells. *Cancer* 92: 500-509, 2001.
- Yang DM, Huang CC, Lin HY, Tsai DP, Kao LS, Chi CW and Lin CC: Tracking of secretory vesicles of PC12 cells by total internal reflection fluorescence microscopy. *J Microsc* 209: 223-227, 2003.
- Schofl C, Rossig L, Mader T, Borger J, Potter E, von zur MA and Brabant G: Impairment of ATP-induced  $\text{Ca}^{2+}$  -signalling in human thyroid cancer cells. *Mol Cell Endocrinol* 133: 33-39, 1997.
- Vanoverberghe K, Mariot P, Vanden Abeele F, Delcourt P, Parys JB and Prevarskaya N: Mechanisms of ATP-induced calcium signaling and growth arrest in human prostate cancer cells. *Cell Calcium* 34: 75-85, 2003.
- Gilbert JA, Bakowski D and Parekh AB: Energized mitochondria increase the dynamic range over which inositol 1,4,5-trisphosphate activates store-operated calcium influx. *EMBO J* 20: 2672-2679, 2001.

- 28 Hoth M, Fanger CM and Lewis RS: Mitochondrial regulation of store-operated calcium signaling in T lymphocytes. *J Cell Biol* 137: 633-648, 1997.
- 29 Gilbert JA and Parekh AB: Respiring mitochondria determine the pattern of activation and inactivation of the store-operated  $Ca^{2+}$  current  $I_{CRAC}$ . *EMBO J* 19: 6401-6407, 2000.
- 30 Rizzuto R, Pinton P, Carrington W, Fay FS, Fogarty KE, Lifshitz LM, Tuft RA and Pozzan T: Close contacts with the endoplasmic reticulum as determinants of mitochondrial  $Ca^{2+}$  responses. *Science* 280: 1763-1766, 1998.
- 31 Boissier S, Magnetto S, Frappart L, Cuzin B, Ebetino FH, Delmas PD and Clezardin P: Bisphosphonates inhibit prostate and breast carcinoma cell adhesion to unmineralized and mineralized bone extracellular matrices. *Cancer Res* 57: 3890-3894, 1997.
- 32 Boissier S, Ferreras M, Peyruchaud O, Magnetto S, Ebetino FH, Colombel M, Delmas P, Delaisse JM and Clezardin P: Bisphosphonates inhibit breast and prostate carcinoma cell invasion, an early event in the formation of bone metastases. *Cancer Res* 60: 2949-2954, 2000.
- 33 Brigham DE, Little G, Lukyanenko YO and Hutson JC: Effects of clodronate-containing liposomes on testicular macrophages and Leydig cells *in vitro*. *J Endocrinol* 155: 87-92, 1997.
- 34 Raiman J, Niemi R, Vepsalainen J, Yritys K, Jarvinen T and Monkkonen J: Effects of calcium and lipophilicity on transport of clodronate and its esters through Caco-2 cells. *Int J Pharm* 213: 135-142, 2001.
- 35 Selander KS, Monkkonen J, Karhukorpi EK, Harkonen P, Hannuniemi R and Vaananen HK: Characteristics of clodronate-induced apoptosis in osteoclasts and macrophages. *Mol Pharmacol* 50: 1127-1138, 1996.
- 36 Buiting AM, Zhou F, Bakker JA, van Rooijen N and Huang L: Biodistribution of clodronate and liposomes used in the liposome mediated macrophage 'suicide' approach. *J Immunol Methods* 192: 55-62, 1996.
- 37 Fromigie O, Lagneaux L and Body JJ: Bisphosphonates induce breast cancer cell death *in vitro*. *J Bone Miner Res* 15: 2211-2221, 2000.
- 38 Lehenkari PP, Kellinsalmi M, Napankangas JP, Ylitalo KV, Monkkonen J, Rogers MJ, Azhayev A, Vaananen HK and Hassinen IE: Further insight into mechanism of action of clodronate: inhibition of mitochondrial ADP/ATP translocase by a nonhydrolyzable, adenine-containing metabolite. *Mol Pharmacol* 61: 1255-1262, 2002.
- 39 Monkkonen H, Moilanen P, Monkkonen J, Frith JC, Rogers MJ and Auriola S: Analysis of an adenine nucleotide-containing metabolite of clodronate using ion pair high-performance liquid chromatography-electrospray ionisation mass spectrometry. *J Chromatogr B Biomed Sci Appl* 738: 395-403, 2000.

*Received January 19, 2004*

*Revised March 24, 2004*

*Accepted April 20, 2004*